

yielded positions for the rest of the nonhydrogen atoms. Several cycles of full-matrix isotropic least-squares refinement were carried out. Standard values for the atomic scattering factors including corrections for anomalous dispersion were employed throughout the structure analysis.²² Thermal parameters for the methyl groups (1C(8) and 2C(8)) and the nitrosyl groups attached to 1Re(1) and 1Re(2) were excessive. A difference electron density map calculated with these methyl and nitrosyl atoms removed revealed positions consistent with disorder between the methyl and nitrosyl groups. The disordered positions were included in the model along with a constrained occupation factor for the disorder in each of the molecules. Constrained least-squares refinements were carried out using the program RAELS.²³ Idealized hydrogen atom positions were included for all hydrogens except those on the trimethylphosphine ligands. Each of the trimethylphosphine ligands was assumed to possess a reorientable thermal liberation axial system (TL model).²⁴

(22) Atomic form factors were from: Cromer, D. T.; Mann, J. B. "International Tables for X-Ray Crystallography"; Kynoch Press: Birmingham, England, 1974; Vol. 4, pp 99-101, Table 2.2B. The atomic form factor for hydrogen was from: Stewart, R. F.; Davidson, E. R.; Simpson, W. T. *J. Chem. Phys.* 1965, 42, 3175.

(23) Rae, A. D. "RAELS, A Comprehensive Constrained Least Squares Program", University of New South Wales, Australia, 1976.

(24) Rae, A. D. *Acta Crystallogr., Sect. A* 1975, A 31, 560.

Least-squares refinement of this model using both strict²⁴ and slack²⁵ constraints converged with discrepancy indices $R_1 = \sum |F_o| - |F_c| / \sum |F_o| = 0.060$ and $R_2 = [\sum w(|F_o| - |F_c|)^2 / \sum w(F_o)^2]^{1/2} = 0.095$. The conventional R factor for the 47 data with $\sin \theta / \lambda < 0.1$ was 0.065. The final difference electron density map was featureless except for several peaks near the Re atoms. Additional X-ray tables for 13 are given in the supplementary material.

Acknowledgment. Support from the Department of Energy, Division of Basic Energy Sciences, is gratefully acknowledged.

Registry No. 1, 80668-22-0; 4, 38814-45-8; 5, 74964-69-5; 6, 80668-21-9; 8, 85283-03-0; 9, 85283-04-1; 10, 96041-43-9; 11, 96055-57-1; 13, 96041-44-0; 14, 38814-46-9; 15, 96094-62-1; 16, 96041-45-1; acetone, 67-64-1; 2-butanone, 78-93-3; cyclopentadiene, 542-92-7.

Supplementary Material Available: Listing of bond lengths, bond angles, atomic coordinates, associated thermal parameters, and the final observed and calculated structure amplitudes ($\times 10$) (37 pages). Ordering information is given on any current masthead.

(25) Waser, J. *Acta Crystallogr.* 1963, 16, 1091. Rae, A. D. *Acta Crystallogr., Sect A* 1978, A 34, 578.

Synthesis and Geometry Determination of Cofacial Diporphyrins. EPR Spectroscopy of Dicopper Diporphyrins in Frozen Solution

Sandra S. Eaton,*^{1b} Gareth R. Eaton,*^{1c} and C. K. Chang*^{1a}

Contribution from the Departments of Chemistry, Michigan State University, East Lansing, Michigan 48824, University of Colorado at Denver, Denver, Colorado 80202, and University of Denver, Denver, Colorado 80208. Received November 2, 1984

Abstract: Frozen solution EPR spectra have been obtained for the dicopper complexes of six covalently linked diporphyrins whose synthesis is also described. The distance between the copper atoms in the diporphyrins was determined from the ratio of the intensity of the half-field transitions to the intensity of the allowed transitions and by computer simulation of the spectra. The values obtained by the two methods were in good agreement and ranged from 4.1 to 5.6 Å. The porphyrin planes were parallel within experimental uncertainty. The angle between the interspin vector and the normal to the porphyrin planes (slip angle) was determined by computer simulation of the spectra and values ranged from 20° to 45°. For the majority of the diporphyrins the separation between the porphyrin planes was 3.9 ± 0.1 Å. In an anthracene pillared diporphyrin the interplanar separation was 4.6 Å. These results were compared with those determined from crystal structures. Although there was no short bond pathway between the two copper atoms, the simulations of the spectra indicated that the absolute value of the copper-copper exchange interaction, J , was >0.3 cm⁻¹.

Binuclear metal complexes capable of coordinating and mediating electron transfer to dioxygen have become an important research area in contemporary bioinorganic chemistry. One class of such complexes is the dimeric porphyrins covalently linked in a cofacial configuration, the metal complexes of which are expected to be able to catalyze the 4-electron reduction of dioxygen to water in a manner possibly related to the terminal oxidase of the respiratory chain: cytochrome *c* oxidase.² The realization of this goal may also lead to the development of inexpensive electrode materials for electroreduction of dioxygen, which is of significant value to fuel cell technology.³

Cofacially linked dimeric porphyrins have been synthesized since 1977.⁴ While variations now exist, one approach that has been

used frequently is the double amide strapping of two diametrically substituted porphyrins.⁵ This method, reported originally by one of the authors, provides a versatile approach to the synthesis of numerous diporphyrins with variable inter-ring distances. Such structural variability proved to be critical in directing the course of interactions between dioxygen and metalodiporphyrins. For example, binuclear cobalt and iron complexes of diporphyrins with five-, six-, and seven-atom linkages (DP-5, DP-6, DP-7) have been tested for their electroreduction response toward dioxygen when coated on a graphite electrode.⁶ Invariably, peroxide was produced in these early investigations; the 4-electron process was not observed. In 1979 Collman and co-workers, using the same synthetic approach, obtained structurally equivalent face-to-face diporphyrins (FTF5 and FTF6).⁷ Additionally they prepared

(1) (a) Michigan State University. (2) University of Colorado at Denver. (c) University of Denver.

(2) Chang, C. K. In "Biochemical and Clinical Aspects of Oxygen"; Caughey, W. S., Ed.; Academic Press: New York, 1979; pp 437-454.

(3) (a) Collman, J. P.; Elliott, C. M.; Halbert, T. R.; Tovrog, B. S. *Proc. Natl. Acad. Sci. U.S.A.* 1977, 74, 18-21. (b) Jahnke, H.; Schonborn, M.; Zimmermann, G. *Top. Curr. Chem.* 1976, 61, 133-181.

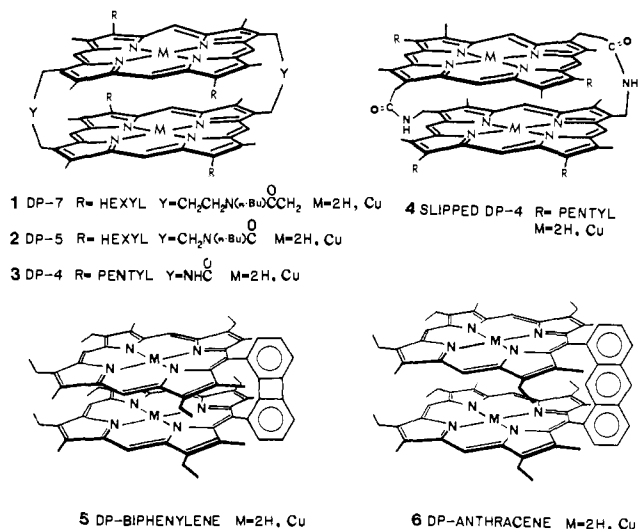
(4) For a review: Dolphin, D.; Hiom, J.; Paine, J. B. *Heterocycles* 1981, 16, 417-447.

(5) (a) Chang, C. K.; Kuo, M.-S.; Wang, C.-B. *J. Heterocycl. Chem.* 1977, 14, 943-945. (b) Chang, C. K. *J. Heterocycl. Chem.* 1977, 14, 1285-1288.

(6) Chang, C. K. *Adv. Chem. Ser.* 1979, 173, 162-177.

FTF4 with shorter connecting chains.⁷ It was during the investigation of the dicobalt FTF4, Anson and collaborators demonstrated the extraordinary ability of this complex to promote the 4-electron reduction of dioxygen on graphite electrode.^{7,8} This ability is not shared by other amide-linked diporphyrins despite the fact that other systems, particularly the Co₂DP-5 (or FTF5), display almost the same oxygen binding properties as Co₂DP-4 in nonaqueous solutions.⁹ Recently another type of cobalt diporphyrin containing only one rigid "pillar" between the two porphyrin rings has become available¹⁰ and it has been shown that they are very effective catalysts for the 4-electron oxygen reduction.¹¹ Interestingly, in this system the catalytic activity was not critically dependent on the length of the spacer arm that separates the two rings. It is evident that our present knowledge on these compounds is still inadequate to interpret their behavior.

There seems little doubt that the unusual catalytic ability of some cobalt diporphyrins is related to certain structural features or special arrangements of the rings not possessed by other diporphyrins. Unfortunately accurate crystal structures of diporphyrins are not always attainable, and therefore alternative methods are needed (or even preferable) for probing the metal-metal distance and diporphyrin geometry in solution. Attempts have been made to estimate the interplanar separation from the value of $2D$ in the frozen solution EPR spectra of copper-copper diporphyrins.^{2,5b,9,10b} However, this method can only give the interspin distance, r . To determine the interplanar separation it is necessary to know the angle between the interspin vector and the normal to the porphyrin planes (the slip angle) as well as r . Furthermore, the determination of r from the value of $2D$ is not reliable if the dipolar interaction is of the same order of magnitude as the nuclear hyperfine splitting and the interspin vector does not coincide with a principal axis of the nuclear hyperfine tensor.¹² Thus computer simulation of the EPR spectra may be required to obtain the interspin distance as well as the lateral displacement of the rings.¹² The interspin distance can also be obtained from the intensity of the half-field transitions.¹² In this paper we have used both methods to probe the structural features of a set of copper diporphyrins 1-6 ($M = \text{Cu}^{\text{II}}$). The electrocatalytic re-



(7) (a) Collman, J. P.; Marrocco, M.; Denisevich, P.; Koval, C.; Anson, F. C. *J. Electroanal. Chem.* **1979**, *101*, 117-122. (b) Collman, J. P.; Denisevich, P.; Konai, Y.; Marrocco, M.; Koval, C.; Anson, F. C. *J. Am. Chem. Soc.* **1980**, *102*, 6027-6036.

(8) Durand, R. R.; Bencosme, C. S.; Collman, J. P.; Anson, F. C. *J. Am. Chem. Soc.* **1983**, *105*, 2710-2718.

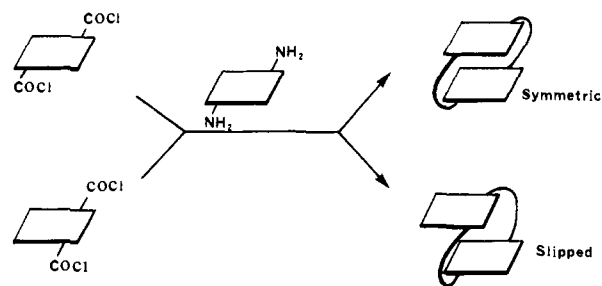
(9) Liu, H. Y.; Weaver, M. J.; Wang, C.-B.; Chang, C. K. *J. Electroanal. Chem.* **1983**, *145*, 439-447.

(10) (a) Chang, C. K.; Abdalmuhdi, I. *J. Org. Chem.* **1983**, *48*, 5388-5390. (b) Chang, C. K.; Abdalmuhdi, I. *Angew. Chem., Int. Ed. Engl.* **1984**, *23*, 164-165.

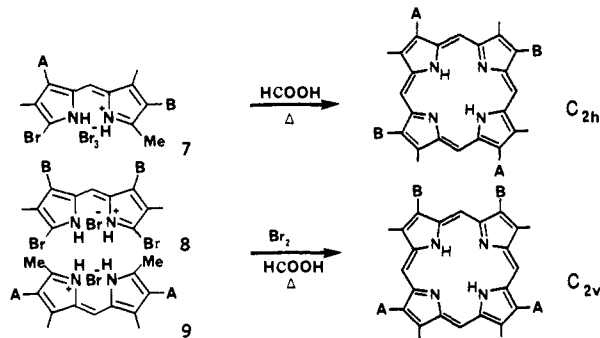
(11) (a) Chang, C. K.; Liu, H. Y.; Abdalmuhdi, I. *J. Am. Chem. Soc.* **1984**, *106*, 2725-2726. (b) Liu, H. Y.; Abdalmuhdi, I.; Chang, C. K.; Anson, F. C. *J. Phys. Chem.* **1985**, *89*, 665-670.

(12) Eaton, S. S.; More, K. M.; Sawant, B. M.; Eaton, G. R. *J. Am. Chem. Soc.* **1983**, *105*, 6560-6567.

Scheme I



Scheme II



sponse toward O₂ reduction by the cobalt complexes of this set of dimers has been documented previously.¹³ The purpose here is 2-fold. We hope to identify, via analogy and extrapolation, any geometric characteristics that correlate with the electrocatalytic properties of the cobalt system. By selecting a set of copper dimers with diverse geometry, we also provide a useful calibration for short interspin distances of the half-field transition method of determining distances. The geometric information derived from this study will be important to the understanding of ligand coordination behavior of all metallodiporphyrins. Also we report here our experience during the design and synthesis of the amide-linked diporphyrins.

Synthesis

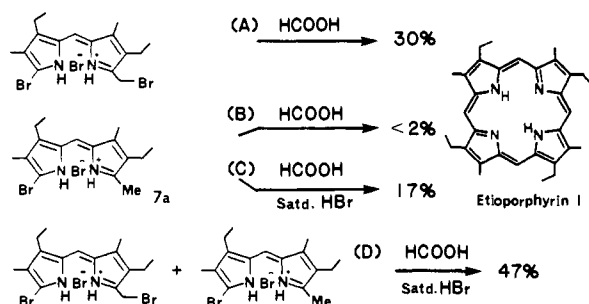
The general strategies of preparing diporphyrins 1-6 have been outlined previously,^{5,10} but with the exception of 6, experimental procedures of synthesis have not been published before. As shown in Scheme I, the amide-linked cofacial dimers 1-3 were synthesized by coupling of diametrically substituted porphyrin diacid chlorides and diamines. When the C_{2h} symmetry of the porphyrin was replaced by a C_{2v} symmetry, the same coupling reaction resulted in a diporphyrin of slipped configuration. Due to the nonequivalence of the two faces of the porphyrin, these couplings invariably yielded two diastereomers (syn and anti), each in turn, consisted of a pair of enantiomers. We have shown in one instance that by crystallization it is possible to isolate one isomer.¹⁴ Separation of the two isomers by HPLC has been successful only with the free base DP-4 and a singly metalated copper-free base DP-5 (prepared by coupling of free base diacid chloride and copper(II) porphyrin diamine). The proportion of the two isomers varied somewhat from batch to batch. The electrochemical properties as well as the absorption and EPR spectra did not give evidence for more than one species, suggesting that the metal-metal distance and overall geometry is not very different for the syn and anti isomers.

The synthesis of C_{2h} and C_{2v} derivatized porphyrins required for the amide couplings is outlined in Scheme II. While the use of brominated dipyrromethenes for porphyrin formation was originally established in Fischer's laboratories,¹⁵ a considerably

(13) See ref 9, ref 11, and: Liu, H. Y. Ph.D. Dissertation, Michigan State University, East Lansing, 1982.

(14) Hatada, M. H.; Tulinsky, A.; Chang, C. K. *J. Am. Chem. Soc.* **1980**, *102*, 7115-7116.

Scheme III



improved procedure has been introduced by Smith.¹⁶ In 1972, Smith demonstrated that when the HBr_3 salt of a 5-bromo-5'-methyl-dipyrromethene **7** ($A = B = \text{Et}$) is heated under reflux in anhydrous formic acid, yields up to 60% of etioporphyrin I can be obtained. He further showed that the extra bromine contained in the perbromide may be substituted by 1 equiv of free bromine without depressing the yield. We have adopted this serviceable approach, with additional improvements, to prepare both C_{2h} and C_{2v} porphyrins since 1976.^{17,18} This route was also employed independently by Battersby for the synthesis of porphyrin models.¹⁹ We introduced a one-pot procedure (see Experimental Section) for dipyrromethene condensation/bromination/porphyrin formation, eliminating the messy and often ruinous manipulations on dipyrromethenes,¹⁷ and established the optimum stoichiometry of free bromine required during the porphyrin cyclization.

When 3,4'-diethyl-4,3'-dimethyl-5-bromo-5'-methyl-2,2'-dipyrromethene hydrobromide (**7a**) is heated in formic acid, the yield of the resultant etioporphyrin I depends critically on the amount of free bromine added at the onset of reaction: the yield rises rapidly from practically zero at zero concentration of bromine to a maximum of 50% at about 0.5 equiv of bromine and then decreases to near 25% at 1 equiv of bromine (vs. **7a**). The yield drops drastically when bromine is present in excess of 1 equiv. The bromine present in this reaction, either as perbromide or as free bromine, according to Smith¹⁶ may serve two purposes: (a) an in situ dehydrogenation agent to oxidize the initially formed porphyrinogen and/or (b) a highly efficient method for the transformation of the 5-bromo-5'-methyl-dipyrromethene into its 5'-(bromomethyl) derivative. Our observation that the best result is achieved with less than 1 equiv of bromine suggests that the role bromine plays could be more intriguing. To aid explanation, four reactions are compared in Scheme III. Reaction A duplicates the original Fischer's condition and indicates that surely the dibromo derivative is a reactive precursor, albeit the yield is not the highest. Reactions B and C demonstrate an important fact: the monobromo compound cannot give substantial yields of porphyrin in boiling formic acid without the aid of HBr. Reaction D then simulates what would be expected if 0.5 equiv of bromine is needed to convert one-half of the 5'-methyl-dipyrromethene to the dibromo derivative. Indeed reaction D has the best yield. We suggest the following events: free bromine brominates half of the 5-bromo-5'-methyl-dipyrromethene into the corresponding 5'-bromomethyl compound and at the same time releases into the reaction medium HBr that assists the subsequent ring closure of the 1-bromo-19-methylbiladiene. If one assumes that the condensation between dipyrromethenes proceeds via an electrophilic attack on the bromopyromethene by the pyrrole CH_2^+ cation, the dibromo derivative should be eminently more suitable than the monobromo compound to undergo porphyrin cyclization, yet it is not the case. The question why reaction A gives poorer yields than reaction D is still a matter of speculation. Perhaps the higher

reactivity of the dibromo system also promotes intermolecular condensation to yield polymers so that a tuned-down system such as (D) actually helps the ring formation.

For practical reasons, porphyrin diesters were always synthesized and purified first; they were then transformed into corresponding acid chlorides or amines using standard methods. The presence of the *n*-hexyl or *n*-pentyl side chains greatly enhances the solubility of these porphyrins in dichloromethane. We were able to carry out all amide couplings in this solvent, including the sparingly soluble **21** and **23** to yield DP-4. The elimination of strong coordinating solvents such as pyridine²⁰ has allowed us to prepare mixed-metal diporphyrins by this direct route. Scheme IV summarizes all the pyrrole and porphyrin precursors required for the synthesis of **1-4**. Because of the length of the experimental details, only one representative dimer, DP-4, is described in the Experimental Section; additional experimental procedures, including the synthesis of **5**, are available as supplementary material.

EPR Spectra and Computer Simulations

EPR spectra were obtained on a Varian E9. Data were collected digitally with a Varian 620/L103 minicomputer. Spectra were obtained at microwave powers that did not cause saturation of the signal. To improve the signal-to-noise ratio of the spectra of the half-field transitions, modulation amplitudes up to one-half of the peak-to-peak line widths were used. Although the use of such large modulation amplitudes causes slight distortion of the line shape, it does not distort the transition energies or the integrated intensity of the signal and should have negligible impact on the analysis of the spectra. A weak background signal from the cavity and Dewar insert was subtracted from the spectra of the half-field transitions. The intensities of the transitions were obtained by double integration. Spectra of each of the compounds were run at two to four concentrations between 5×10^{-4} and 3×10^{-3} M. The relative intensity of the half-field transitions was extrapolated to infinite dilution to correct for intermolecular spin-spin interaction.¹² The change in the relative intensity of the half-field transitions for these samples as a function of concentration was less than 10%.

The spectra were simulated using the computer program MENO²¹ which is a modified version of Smith and Pilbrow's program ALLSYM.²² The Hamiltonian (eq 1) consists of terms for two independent copper electrons 1 and 2 as given in eq 2 and an interaction term as given in eq 3. The interaction term includes

$$\mathcal{H} = \mathcal{H}_1 + \mathcal{H}_2 + \mathcal{H}_{\text{int}} \quad (1)$$

$$\mathcal{H}_i = \sum_j (\beta g_j S_{ij} H_j + A_j S_{ij} I_{ij}) \quad i = 1, 2 \quad j = x_i, y_i, z_i \quad (2)$$

$$\mathcal{H}_{\text{int}} = -JS_1 S_2 + \mathcal{H}_{\text{dipolar}} \quad (3)$$

an isotropic exchange contribution and an anisotropic dipolar contribution. The symbols in eq 1-3 have their usual meanings and are discussed in detail in ref 21. The perturbation calculations were carried to second order. The splitting between the singlet and triplet levels is J and a negative value of J indicates an antiferromagnetic interaction. It was not possible to determine the sign of J from the spectra of the copper-copper diporphyrins.

The Hamiltonian is based on two assumptions concerning the spin-spin interaction. First it is assumed that the point dipole approximation is valid. Nordenskiöld et al. have examined the use of the point dipole approximation for water coordinated to paramagnetic metals. They concluded that it did not work well for the coordinated oxygen but that it caused less than 1% error for the protons.²³ Since there is not a bond between the two copper ions and since the copper-copper distances are greater than the metal-proton distances examined in ref 23, the point-dipole approximation is likely to be adequate for these dimers. Second,

(15) Fischer, H.; Orth, H. "Die Chemie des Pyrrols"; Akademische Verlag: Leipzig, 1937; Vol. 2, Part 1, p 176-183.

(16) Smith, K. M. *J. Chem. Soc., Perkin Trans. 1* **1972**, 1471-1475.

(17) Chang, C. K. *J. Am. Chem. Soc.* **1977**, *99*, 2819-2821.

(18) Paine, J. B.; Chang, C. K.; Dolphin, D. *Heterocycles* **1977**, *7*, 831-838.

(19) Battersby, A. R.; Buckley, D. G.; Hartley, S. G.; Turnbull, M. D. *J. Chem. Soc., Chem. Commun.* **1976**, 879-881.

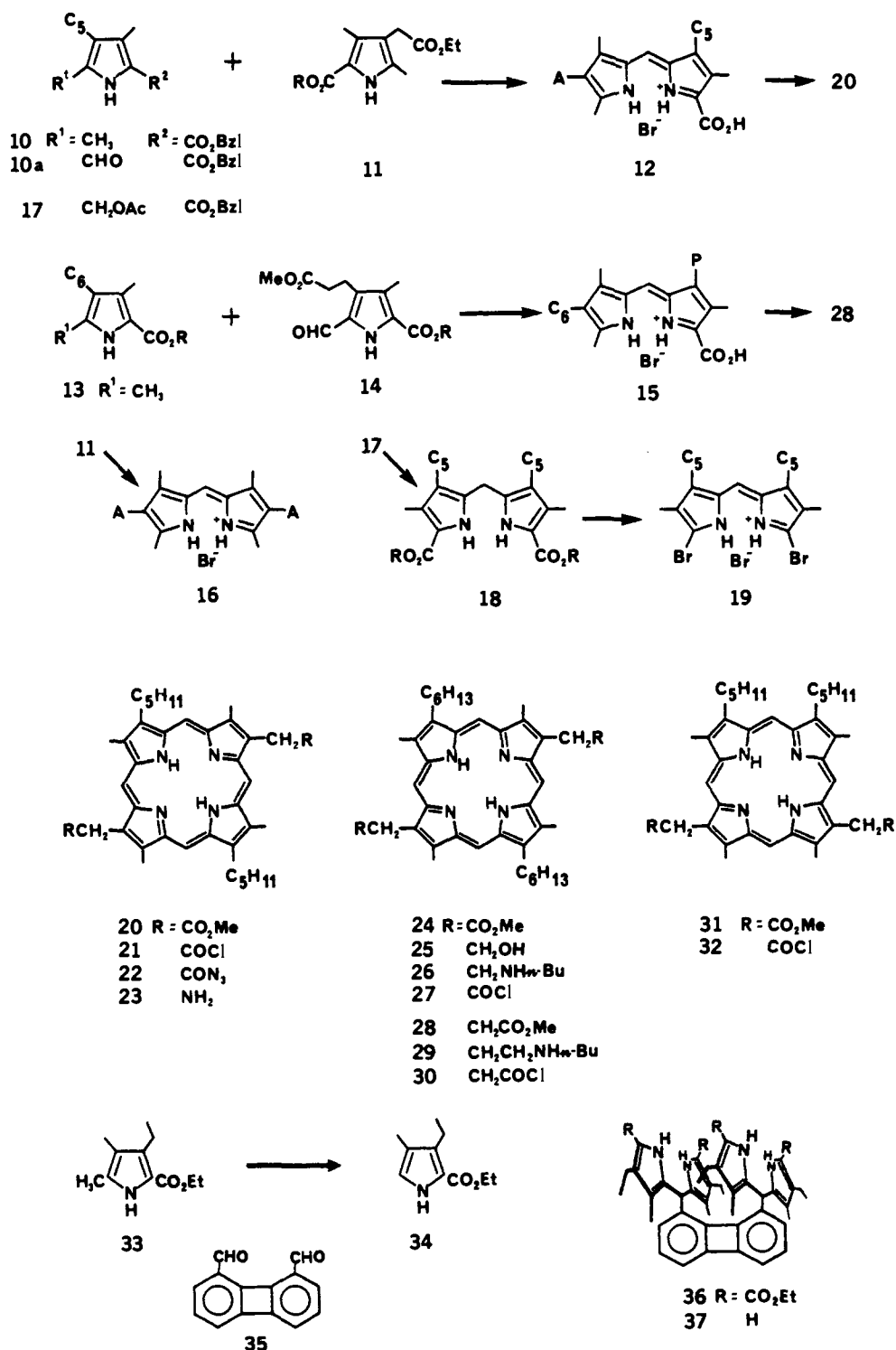
(20) Collman, J. P.; Bencosme, C. S.; Durand, R. R.; Kreh, R. P.; Anson, F. C. *J. Am. Chem. Soc.* **1983**, *105*, 2699-2703.

(21) Eaton, S. S.; More, K. M.; Sawant, B. M.; Boymel, P. M.; Eaton, G. R. *J. Magn. Reson.* **1983**, *52*, 435-449.

(22) Smith, T. D.; Pilbrow, J. R. *Coord. Chem. Rev.* **1974**, *13*, 173-278.

(23) Nordenskiöld, L.; Laaksonen, A.; Kowalewski, J. *J. Am. Chem. Soc.* **1982**, *104*, 379-382.

Scheme IV



it is assumed that the isotropic exchange is sufficiently weak that anisotropic exchange can be neglected.^{12,24} The good agreement between the values of r obtained by EPR and by X-ray crystallography both in this study and in prior studies¹² indicates that this assumption is valid.

The parameters used in the simulations were $g_{\perp} = 2.047\text{--}2.050$, $g_{\parallel} = 2.190\text{--}2.196$, $A_{\perp} = 30 \times 10^{-4} \text{ cm}^{-1}$, and $A_{\parallel} = 205 \times 10^{-4} \text{ cm}^{-1}$. The \mathbf{g} and \mathbf{A} tensors were axial within experimental uncertainty. These parameters are in good agreement with values obtained previously for copper porphyrins in frozen solution²¹ and

single crystals.²⁵ The contributions for ^{63}Cu and ^{65}Cu were not resolved in the spectra so a single isotope was assumed in the calculations. Since the nitrogen hyperfine splitting was not resolved in the spectra, it was not included in the calculations. The large line widths in the experimental spectra (line widths between 40 and 60 G were used in the calculations) no doubt reflect the unresolved nitrogen hyperfine splitting. 56 values of θ (angle between the magnetic field and the z axis of the copper \mathbf{g} and \mathbf{A} tensors) per 180° and 24 values of ϕ (angle between the projection of the magnetic field on the porphyrin plane and the x axis of the

(24) Bleaney, B.; Bowers, K. D. *Proc. R. Soc. London, Ser. A* 1952, 214, 451-456.

(25) Damoder, R.; More, K. M.; Eaton, G. R.; Eaton, S. S. *J. Am. Chem. Soc.* 1983, 105, 2147-2154.

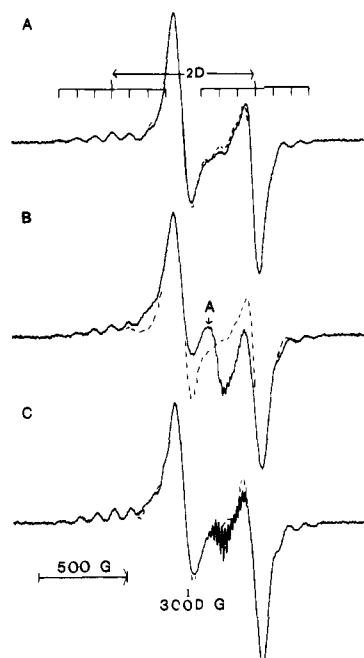


Figure 1. X-band (9.101 GHz) EPR spectra of the allowed transitions for (A) Cu₂DP-4 (3), (B) Cu₂DP-5 (2), and (C) Cu₂DP-B (5) at -180 °C in 1:1 toluene/dichloromethane solution. The spectra were obtained on 1 mM solutions with 1-mW microwave power and 4-G modulation amplitude. The peak marked "A" was attributed to aggregated material. The dotted lines indicate regions in which the calculated curves do not overlay the experimental data.

copper *g* and *A* tensor) per 180° were used in the calculations. Typical calculations required about 5 min of VAX 780 CPU time for the allowed transitions and 2 min for the half-field transitions.

The spectra of the half-field transitions were analyzed as follows. The value of the spin-spin distance, *r*, was obtained from the ratio of the intensity of the half-field transitions to the intensity of the allowed transitions. The spectra of the half-field transitions are independent of the values of *r* and *J* (exchange interaction) for the range of values encountered in this study. The spectra are determined by the relative orientations of the interspin vector and the *g* and *A* tensors for the two copper ions. All of the spectra were consistent with parallel *z* axes for the *g* and *A* tensors of the two copper ions, which indicated that the porphyrin planes were parallel. Since the *g* and *A* tensors were axial, no information could be obtained concerning the rotation around the *z* axis of one porphyrin relative to the other. The value of ϵ was adjusted to obtain the best fit to the half-field spectra. The uncertainties in ϵ were $\pm 10^\circ$. The positions of the lines in the spectra of the allowed transitions are dependent on the values of *r*, *J*, and ϵ . Therefore the values of *r* and ϵ obtained from the half-field transitions were used as the starting parameters for the simulations of the allowed transitions. The positions of the lines in the parallel portion of the spectra could not be matched with values of *J* less than 0.3 cm⁻¹. The appearance of the spectra is independent of the value of *J* for *J* > 0.3 cm⁻¹ so only a lower limit could be obtained. The positions of the turning points in the spectra are dependent on *r* and ϵ . If the value of ϵ is incorrect, it is not possible to simultaneously match the splittings in the parallel and perpendicular portions of the spectra. The values of ϵ obtained from the allowed transitions agreed well with the values obtained from the half-field transitions. On the basis of the sensitivity of the simulated spectra to changes in the value of *r* and uncertainties in the relative intensities of the half-field transitions, the uncertainties in *r* ranged from ± 0.05 Å at *r* = 4.1 Å to ± 0.1 Å at *r* = 5.7 Å.

Spectra and Assignments

The EPR spectrum of the allowed transitions for copper-copper diporphyrin 3 in frozen solution is shown in Figure 1A. The dipolar splitting of both the copper parallel and perpendicular lines

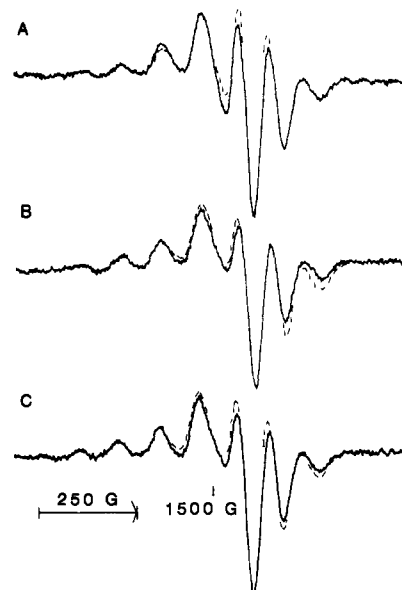


Figure 2. X-band EPR spectra of the half-field transitions for (A) Cu₂DP-4 (3), (B) Cu₂DP-5 (2), and (C) Cu₂DP-B (5) at -180 °C in 1:1 toluene/dichloromethane solution. The spectra were obtained on 1 mM solutions with 20-mW microwave power and 16-G modulation amplitude. The overall amplification of the spectra in this figure is about 35 times that for Figure 1. The dotted lines indicate regions in which the calculated curves do not overlay the experimental data.

was well resolved. The simulated spectrum shown in Figure 1A was obtained with *r* = 4.15 Å, *|J|* = 0.5 cm⁻¹, and ϵ = 15°. The value of 2*D* read from the splitting of the copper parallel lines (800 G) corresponds to *r* = 4.2 Å. The spectrum of the half-field transitions for 3 is shown in Figure 2A. The nuclear hyperfine splitting by the two copper ions was well resolved as expected for copper porphyrin dimers.²² The ratio of the intensity of the half-field transitions to the intensity of the allowed transitions was 4.6×10^{-3} , which corresponds to *r* = 4.04 Å.¹² This value agrees well with the values obtained from 2*D* and by computer simulation of the allowed transitions. The simulated spectrum was obtained with ϵ = 15°.

The EPR spectra of the allowed and forbidden transitions for copper-copper diporphyrin 2 in frozen solution are shown in Figures 1B and 2B, respectively. The spectra were similar to those of copper-copper diporphyrin 3. The peak at about 3100 G that is marked "A" in Figure 1B was strongly concentration dependent and is attributed to aggregation of the porphyrin. Although the intensity of that signal decreased as the concentration was decreased, the intensity did not extrapolate to zero at infinite dilution. This suggests that a small amount of polymeric material may be present in the sample. The spectrum in 1B is in good agreement with the previously published spectra of this compound although the spectrum in 2B does not agree with the previously published spectra.^{5,6} The earlier spectra reported for the half-field signal were apparently due to ferric ion impurities in the quartz sample tubes which largely obscured the half-field transitions of the copper-copper diporphyrin. The simulated spectra were obtained with *r* = 4.15 Å, *|J|* = 0.5 cm⁻¹, and ϵ = 20°. The value of 2*D* obtained from the copper parallel lines (820 G) corresponds to *r* = 4.2 Å. The relative intensity of the half-field transitions was 4.1×10^{-3} . This gives *r* = 4.12 Å, which is in good agreement with the values obtained from the allowed transitions.

Some comment is necessary concerning the impact of aggregation on the intensity of the half-field transitions. The intensity of the half-field transition is determined by the magnitude of dipolar interactions, either inter- or intramolecular. In these samples the fraction of the material that was aggregated was small, which tended to minimize the contribution of the aggregated material to the half-field transitions. Since the effect of the dipolar spin-spin interaction on the intensity of the half-field transitions depends on *r*⁻⁶, even a small amount of aggregation could sig-

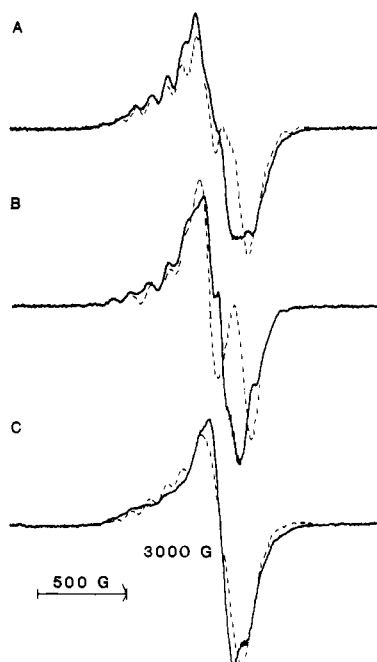


Figure 3. X-band EPR spectra of the allowed transitions for (A) Cu₂DP-7 (**1**) (B) Cu₂DP-A (**6**), and (C) slipped Cu₂DP-4 (**4**) at -180 °C in 1:1 toluene/dichloromethane solution. The spectra were obtained under conditions identical with those described in Figure 1.

nificantly alter the relative intensity of the half-field transitions if the interspin distance in the aggregated material were much shorter than the intramolecular spin-spin distance. However, in these diporphyrins the distance of closest approach of the two copper ions in the aggregated material is about 3.5 Å,¹⁴ which is only slightly shorter than the intramolecular spin-spin distance. Therefore a small amount of aggregation would not be expected to have a major impact on the relative intensity of the half-field transitions. The small concentration dependence of the relative intensity of the half-field transitions and the good agreement between the values of r obtained by computer simulation of the allowed transitions and from the relative intensity of the half-field transitions confirms that the impact of aggregation on the intensity of the half-field transitions was negligible in these cases. Note that aggregation is significantly more important if the intramolecular distance to be measured is longer.

Figures 1C and 2C show the allowed and half-field transitions, respectively, for copper-copper diporphyrin **5**. The spectra were similar to the spectra of **3** and **2**. The sharp lines between 3100 and 3200 G in Figure 1C were due to a small amount of monomeric copper porphyrin or to diporphyrin that had copper coordinated to only one of the porphyrins. The spectrum in Figure 1C is in good agreement with the figure in ref 10b although the spectrum in Figure 2C does not agree with that previously reported.^{10b} As discussed above, the previously reported half-field transition was apparently due to a ferric ion impurity in the sample tube. The simulated spectra were obtained with $r = 4.13$ Å, $|J| = 0.5$ cm⁻¹, and $\epsilon = 20^\circ$. The value of $2D$ obtained from the copper parallel lines (820 G) corresponds to $r = 4.2$ Å. The relative intensity of the half-field transitions was 4.0×10^{-3} , which corresponds to $r = 4.14$ Å. An X-ray crystal structure of this complex, obtained after the EPR studies were completed, gave a Cu-Cu distance of 3.81 Å,²⁶ which indicates substantial similarity between the structures in solution and the single crystal.

The allowed and half-field transitions for copper-copper diporphyrin **1** are shown in Figures 3A and 4A, respectively. The smaller splittings of the allowed transitions for **1** than for **3**, **2**, or **5** indicated a longer interspin distance. Due to the weaker dipolar interaction, the copper parallel lines on the high-field side

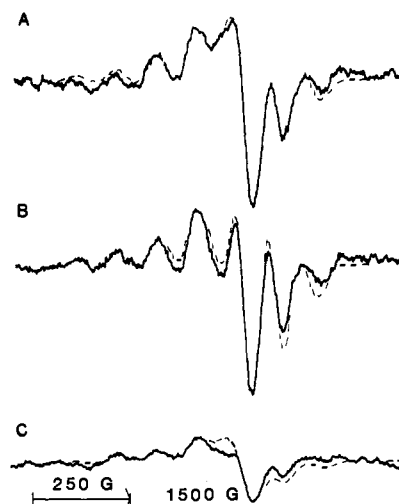


Figure 4. X-band EPR spectra of the half-field transitions for (A) Cu₂DP-7 (**1**), (B) Cu₂DP-A (**6**), and (C) slipped Cu₂DP-4 (**4**) at -180 °C in 1:1 toluene-dichloromethane solution. The spectra were obtained in 1 mM solutions with 200-mW microwave power and 16-G modulation amplitude. The overall amplification of the spectra in this figure is about 100 times that for Figure 3 and 3 times that for Figure 2. The dotted lines indicate regions in which the calculated curves do not overlay the experimental data.

of the spectrum were poorly resolved, which precluded an estimate of the value of $2D$. The simulated spectrum was obtained with $r = 4.95$ Å, $|J| = 0.5$ cm⁻¹, and $\epsilon = 40^\circ$. The major discrepancy between the observed and calculated spectra in Figure 3A was at about 3100 G, which is at the position of the peak assigned to aggregated material in Figure 1B. This region of the spectrum was concentration dependent, which suggests that the discrepancy was due to aggregation. The relative intensity of the half-field transitions was 1.3×10^{-3} , which corresponds to $r = 5.0$ Å. The X-ray crystal structure of **1** gave a copper-copper distance of 5.22 Å and a slip angle of 46.4°.²⁷ Thus the EPR results indicate that the structure in frozen solution is similar to that observed in the single crystal. It should be noted that both the larger copper-copper distance and the larger value of ϵ are consistent with slightly greater slip of one porphyrin plane relative to the other in the crystal than in the frozen solution.

The spectra of **6** (Figures 3B and 4B) were similar to the spectra of **1**. The simulated spectra were obtained with $r = 4.95$ Å, $|J| = 0.5$ cm⁻¹, and $\epsilon = 20^\circ$. The discrepancy between the observed and calculated spectra at approximately 3100 G was attributed to aggregation of a small amount of the sample. The relative intensity of the half-field transitions (1.4×10^{-3}) gave $r = 4.9$ Å. An X-ray crystal structure of the nickel-nickel analogue of **6** gave a metal-metal distance of 4.57 Å and $\epsilon = 20^\circ$.²⁶ Thus the EPR data for this diporphyrin again indicate substantial similarity between the structures in the crystal and in frozen solution.

The allowed and half-field transitions for copper-copper diporphyrin **4** are shown in Figures 3C and 4C, respectively. The simulated spectra were obtained with $r = 5.5$ Å, $|J| = 0.5$ cm⁻¹, and $\epsilon = 45^\circ$. The discrepancy between the observed and calculated spectra in the vicinity of 3100 G was again attributed to a small amount of aggregation. There was some dependence of the experimental line widths of the copper parallel lines on the nuclear spin that was not included in the simulated spectra. The low-field lines in the simulated spectrum were sharper than the experimental lines although the same line width gave good agreement with the high-field side of the spectrum. It should be noted that due to the differences between the values of ϵ for the spectra in Figures 3B and 3C, the copper parallel lines in Figure 3C extend to almost as low field as in Figure 3B despite the fact that r is substantially

(26) Fillers, J. P.; Ravichandran, K. G.; Rydel, T.; Abdalmuhdi, I.; Tulinsky, A.; Chang, C. K., manuscript submitted.

(27) The intramolecular slip angle reported in ref 14 should have been 46.4° and the intermolecular slip angle should have been 43.5°. See correction: Hatada, M. H.; Tulinsky, A.; Chang, C. K. *J. Am. Chem. Soc.* **1981**, *103*, 5623.

Table I. Distances and Angles Obtained for Dicopper Diporphyrins

diporphyrin	r , Å		ϵ , deg ^c	interplanar ^d separation	% H ₂ O ₂ ^e
	half-field ^a	simulation ^b			
DP-4 (3)	4.04	4.15	15	4.0	<5
DP-5 (2)	4.12	4.15	20	3.9	>40
DP-7 (1)	5.0 (5.22) ^f	4.95	40	3.8 (3.52) ^f	>60
DP-B (5)	4.14 (3.81)	4.13	20	3.9 (3.5)	4
DP-A (6)	4.9 (4.57)	4.9	20	4.6 (3.9)	4
slip-4 (4)	5.7	5.5	45	3.9	>60

^aCopper-copper distances obtained from the relative intensity of the half-field transitions. ^bCopper-copper distances obtained by simulation of the allowed transitions. ^cAngle between the z axes of the copper g and A tensors and the interspin vector. ^dSeparation between the two parallel porphyrin planes. ^ePercentage of formation of hydrogen peroxide evaluated from %H₂O₂ = $-i_R/(Ni_D)$ where i_R and i_D are ring and disc limiting current, respectively, and N (=0.182) is the collection coefficient. These data were measured by using dicobalt diporphyrins coated on the graphite disk of a ring-disc electrode immersed in O₂-saturated 0.5 M aqueous trifluoroacetic acid.¹³ ^fValues given in parenthesis are the corresponding crystal structure data; see ref 14 and 26-28. The crystal structures were determined for Cu₂DP-7, Cu₂DP-B, and Ni₂DP-A.

longer for 4 than for 6. This is a good example of the difficulties that arise in attempts to obtain $2D$ from EPR spectra in which the axes of the spin-spin interaction and the hyperfine interaction do not coincide. The relative intensity of the half-field transitions (5.5×10^{-4}) gave $r = 5.7$ Å for 4.

Discussion

The values of the interplanar spacings²⁸ for the six diporphyrins obtained from the values of r and ϵ are included in Table I. For all of the diporphyrins except 6, the interplanar separation was 3.9 ± 0.1 Å. The small range of values for a diversity of bridges between the two porphyrins suggests that this distance may represent an optimal trade-off for porphyrin-porphyrin interactions. Another unmistakable pattern of these diporphyrins is that they all have some slippage. The lateral translations as indicated by the slip angle for dicopper 2, 3, 5, and 6 are relatively small in comparison with dicopper DP-7 (1), which has nearly as large a slippage as dicopper 4. One rationale for the large slippage that occurred in Cu₂DP-7 may be that dimers prefer a relatively short (ca. 3.9 Å) interplanar separation, but to achieve this distance and to simultaneously accommodate the two rather "long" connecting chains, lateral translation is the only solution. A counterargument, however, could be that extensive slippage is an intrinsic property of stacked porphyrins; it is the connecting structure that physically limits the lateral shift attainable in each case. Reality may well lie somewhere in between these two descriptions: i.e., a short interplanar separation and a modest slippage both contribute to a preferred conformation. Recent theoretical calculations on free base porphine dimers indeed suggest that a translated structure with an interplanar separation of 3.7 Å and a lateral shift of 1.4 Å can be quite stable and such a configuration is consistent with the crystal structure.²⁹ From these values one calculates $\epsilon = 21^\circ$. Thus the frozen solution geometries are in reasonable agreement with theoretical calculations even though the preferred interplanar spacing appears to be slightly longer in frozen solution than in the crystal.

The last column of Table I also compares the O₂ electroreduction response of the corresponding cobalt derivatives. There appears to be no relationship between r , ϵ , or interplanar spacing and the effectiveness as 4-electron catalysts. For example, while the three effective 4-electron catalysts 3, 5, and 6 ($M = Co$) have a small slip angle, so does 2. However, for the "pillar" type complexes 5 and 6 we have suggested¹¹ that the rings are flexible

enough to achieve whatever structure is advantageous for the formation and cleavage of the cobalt peroxo intermediate, even to overcome the large discrepancy of r between 5 and 6. The answer to this question may be found when mechanisms of the reduction of the Co-O₂-Co species are fully understood.

For all of the experimental spectra it was only possible to simulate the spectra if the absolute value of J was >0.3 cm⁻¹. Thus, although there was no short bond pathway between the two copper ions, there was an exchange interaction that was large on the X-band EPR scale. Such an interaction could occur via interaction between one copper and a nitrogen coordinated to the second copper or via the π - π interaction between the two porphyrins.

In summary, EPR spectra of all six cofacial diporphyrins indicate good agreement between the values of the copper-copper distance, r , obtained by simulation of the allowed transitions and those calculated from the relative intensity of the half-field vs. allowed transitions. More significantly, for three of the compounds the values of r obtained in frozen solution were similar to values obtained from X-ray crystal structures. Since the measurement of the relative intensity of the half-field transition only requires double integration of the experimental spectra, it is easier to obtain the value of r by this method than by simulation of the allowed transitions. To also determine ϵ and the interplanar spacing it is necessary to simulate the spectra. For five of the diporphyrins the interplanar separation was 3.9 ± 0.1 Å. The absolute value of the exchange interaction between the two copper ions was >0.3 cm⁻¹ for all of the dimers. This set of compounds thus provides a useful calibration for short interspin distances of the half-field transition method of determining distances¹² and demonstrates the power of computer simulation of EPR spectra of interacting spins.

Experimental Section

NMR spectra were obtained in CDCl₃ (unless solvent specified otherwise) with Me₄Si internal standard on a Varian T-60 or a Bruker WM-250 instrument. Chemical shifts were recorded in parts per million. Mass spectra (direct insertion probe, 70 eV, 200-300 °C) were measured with a Finnigan 4021 or a Varian MAT CH-5 mass spectrometer. Elementary analyses were performed by Spang, Ann Arbor, MI, or MicAnal, Tucson, AZ. Visible absorption spectra were measured with a Cary 219 spectrophotometer. Dichloromethane was distilled over calcium hydride. The preparation of compounds was done in MI. EPR spectroscopy and computer simulations were done in Denver.

General Procedures for Porphyrin Synthesis. (1) Catalytic Hydrogenolysis of Pyrrole Benzyl Esters. The appropriate pyrrole ester (0.5 mol) was dissolved in 800 mL of THF in a 2-L round-bottom flask. Palladium on charcoal (10%, 5 g) and a few drops of triethylamine were added before the flask was connected to gas burets. Hydrogenation was carried out under 1 atm of hydrogen with magnetic stirring. After gas uptake had ceased, the solution was filtered and evaporated to give the pyrrole acid in almost quantitative yield. The pyrrole acids should be stored in a refrigerator.

(2) Dipyrromethene Formation and Porphyrin Cyclization. Dimethyl 3,13-Dipentyl-2,7,12,17-tetramethylporphine-8,18-diacetate (20). To a mixture of equal molar equivalents (0.1 mol) of the hydrogenolyzed 10b and 11³⁰ suspended in acetonitrile and methanol (200 mL each) was added all at once a HBr saturated acetic acid solution (ca. 35%, 20 mL), and the mixture was brought to a gentle reflux for 20 min. The deep brown solution was evaporated and dried in vacuo. Anhydrous formic acid (280 mL) was then added to dissolve the residue, followed by 1.6 equiv of bromine (i.e. 0.16 mol, 1 equiv for decarboxylation and 1/2 equiv for bromination of the methyl group). The mixture was heated under reflux in an oil bath maintained at 130-135 °C for 2 h. The condenser was then removed and the solvent was boiled off under air. The black residue was dissolved in methanol (100 mL), the solvent was boiled off again, and the residue redissolved in 100 mL of methanol. Small amounts of trimethyl orthoformate (20 mL) and sulfuric acid (concentrated, 2 mL) were added and the mixture was allowed to stand at room temperature, protected from moisture in the dark, for 1 day. Crystalline porphyrin sometimes separated from the liquid by this time. If so, the crystals were collected by filtration first, and the filtrate was evaporated and the residue loaded onto a silica gel column. A black nonfluorescent

(28) Interplanar separation = $r \cos \epsilon$. Due to the warping of the porphyrin rings observed in crystal structures of 5 and 6, it is rather difficult to define the interplanar distance in these two compounds. The value quoted in Table I are the separation of the mean planes.

(29) Sudhindra, B. S.; Fuhrhop, J.-H. *Int. J. Quantum Chem.* **1981**, *20*, 747-753.

(30) Jackson, A. H.; Kenner, G. W. *J. Chem. Soc., Perkin Trans. I* **1974**, 480.

band was eluted first by dichloromethane and discarded. The porphyrin methyl ester came off with pure dichloromethane but often required 5% methanol/ CH_2Cl_2 to be eluted completely. The main porphyrin fractions were combined and evaporated while the heavily contaminated fractions required a second column. The porphyrin was redissolved in small amounts of CH_2Cl_2 (50 mL) containing formic acid (5 mL) and precipitated by methanol containing 5% triethylamine; yield of **20**, 11 g (18%): mp 221–224 °C; mass spectrum, m/e 650 (M^+), 325 (M^{2+}); UV-vis (CH_2Cl_2) 400 nm, 500, 534, 568, 620; NMR δ -3.95 (br s, 2 H, NH), 0.93 (t, 6 H, pentyl), 1.57 (m, 8 H, pentyl), 2.37 (m, 4 H, $\text{CH}_2\text{C}_3\text{H}_7$), 3.43 (s, 6 H, Me), 3.47 (s, 6 H, Me), 3.70 (s, 6 H, OMe), 3.83 (t, $J = 7.0$ Hz, $\text{CH}_2\text{C}_4\text{H}_9$), 4.80 (s, 4 H, CH_2CO), 9.70 (s, 2 H, meso), 9.77 (s, 2 H, meso). Anal. Calcd for $\text{C}_{40}\text{H}_{50}\text{N}_4\text{O}_4$: C, 73.81; H, 7.74; N, 8.61. Found: C, 73.47; H, 7.58; N, 8.49.

3,13-Dipentyl-2,7,12,17-tetramethylporphyrin-8,18-diacetic Chloride (21). The porphyrin methyl ester **20** (500 mg) dissolved in 88% formic acid (30 mL) and concentrated HCl (5 mL) was heated on a steam bath for 1 h. The solvent was then evaporated under reduced pressure and the residue dried in vacuo to give the porphyrin diacid hydrochloride salt (535 mg). This salt was suspended in POCl_3 (2 mL); oxalyl chloride (3 mL) and CH_2Cl_2 (20 mL) were added after all solids became dissolved. The mixture was heated to reflux under nitrogen for 1 h before the liquid was evaporated under reduced pressure. The dark red residue was dried in vacuo for 1 h, yield 563 mg, IR 1795 cm^{-1} (COCl); it was used immediately without further purification.

3,13-Dipentyl-2,7,12,17-tetramethylporphyrin-8,18-dicarbonyl Azide (22). To a dichloromethane (25 mL) solution of the acid chloride **21** (300 mg) stirred in an ice bath was added all at once a mixture of sodium azide (1 g) and tetrabutylammonium chloride (300 mg) in water (10 mL). After 10 min, dichloromethane was removed under reduced pressure and a black solid was formed in the water phase. The solid was collected by filtration, washed with water, and dried under vacuum. The crude product was purified by chromatography on a short (2 in.) silica gel column, using dichloromethane as eluent, to give the diazide (248 mg, 91% yield): IR 1710, 2135 cm^{-1} ; ^1H NMR δ -4.13 (br s, 2 H, NH), 0.93 (t, 6 H, pentyl), 1.5 (m, 8 H, pentyl), 2.1 (m, 4 H, pentyl), 3.37 (s, 6 H, Me), 3.43 (s, 6 H, Me), 3.86 (t, 4 H, $\text{CH}_2\text{C}_4\text{H}_9$), 4.47 (s, 4 H, CH_2CON_3), 9.77 (s, 4 H, meso).

3,13-Dipentyl-8,18-bis(aminomethyl)-2,7,12,17-porphyrin (23). Azide porphyrin **22** (248 mg) was refluxed under nitrogen in dry benzene (100 mL) for 1 h; after that, benzene was evaporated and the residue was chromatographed on a short silica gel column, eluted with dichloromethane, to yield the diisocyanate (205 mg, 90%), IR 2250 cm^{-1} (NCO). This product was brought to reflux in a mixture of benzene (300 mL) and HCl (6 N, 200 mL) for 1 h. After cooling, the benzene layer was discarded. A mixture of 500 mL of 9:1:0.5 chloroform/methanol/triethylamine was added to the acid solution. To this mixture cooled in an ice bath, 50% NaOH solution was added until it was slightly basic. The organic layer was separated and concentrated to afford 145 mg of the amine **23** (79%): IR 3350 cm^{-1} ; mass spectrum, m/e 564 (M^+); NMR 0.93 (t, 6 H, pentyl), 1.5 (m, 8 H, pentyl), 2.1 (m, 4 H, pentyl), 3.35 (s, 6 H, Me), 3.44 (s, 6 H, Me), 3.82 (t, 4 H, $\text{CH}_2\text{C}_4\text{H}_9$), 5.18 (s, 4 H, CH_2NH_2), 9.88 (s, 4 H, meso). This material was used without further purification for the following coupling reaction.

General Procedure for Preparation of Amide-Linked Diporphyrins. Porphyrin diacid chloride (0.4 mmol) was dissolved in anhydrous di-

chloromethane (60 mL) and transferred to a 100-mL syringe under nitrogen gas. Equal moles of porphyrin diamine were dissolved in 1 mL of dry triethylamine, diluted with dichloromethane (60 mL), and placed in another identical syringe. These two syringes were mounted on a motor-driven syringe pump (Sage 352) and their contents were injected simultaneously through stainless steel needles to a 1-L flask containing 500 mL of dry dichloromethane under vigorous stirring. After the addition was complete (1 h), the mixture was stirred for another hour before the solvent was removed. The residue dissolved in dichloromethane (50 mL) was passed through a silica gel pad; the pad was rinsed with dichloromethane until no more product was eluted. The solution was concentrated before it was charged onto preparative TLC plates (Analtch, 1500- μm silica gel); a solvent mixture of 94:6 $\text{CH}_2\text{Cl}_2/\text{MeOH}$ was used as the developing medium. The diporphyrin band thus collected required one more pass on a fresh plate, developed with 97:3 $\text{CH}_2\text{Cl}_2/\text{MeOH}$, to remove tailing impurities. The diporphyrin was finally purified by crystallization from dichloromethane/methanol.

Diporphyrin-4 (3). This dimer was prepared by reacting **21** and **23** according to the method described above, yield 20–23%: UV-vis ($\text{C}-\text{H}_2\text{Cl}_2$) 377 nm (Soret), 504, 542, 570, 625; mass spectrum, m/e 1150 (M^+) by FAB, in 1-thioglycerol matrix. Anal. Calcd for $\text{C}_{74}\text{H}_{90}\text{N}_{10}\text{O}_2$: C, 77.18; H, 7.88; N, 12.16. Found: C, 77.70; H, 8.13; N, 11.95. ^1H NMR δ -7.9 (br s, 4 H, NH), 0.9 (m, 12 H, pentyl), 1.5 (br, 16 H, pentyl), 1.95 (br, 8 H, pentyl), 3.5–3.7 (4 s, 24 H, Me), 3.9 (m, 8 H, $\text{CH}_2\text{C}_4\text{H}_9$), 4.65 (m, 4 H, CH_2CO), 5.4–6.0 (m, 4 H, CH_2N), 8.6–9.2 (7 s, 8 H, meso). The NMR spectrum of the recrystallized diporphyrin-4 revealed seven meso proton resonances, suggesting that the compound consists of syn and anti isomers. This mixture was separated by HPLC (Waters Radial-Pak, 10- μm silica gel, dichloromethane–3% MeOH) to give two barely separable fractions in ca. 6:4 ratio. The faster moving component showed four meso peaks at 8.68, 8.72, 8.75, and 8.90 ppm, while the other exhibited peaks at 8.73, 8.78, 9.10, and 9.17 ppm. We tentatively assigned the faster component as the anti isomer and the slower one syn. The two compounds showed identical UV-vis spectrum and redox characteristics. The sample used in the present EPR study was obtained from the syn isomer.

Metal Insertions. Copper(II) and cobalt(II) complexes were prepared by addition of a saturated methanolic solution of copper(II) acetate or cobalt(II) acetate, respectively, to a dichloromethane solution of the diporphyrin. A small amount of anhydrous sodium acetate was added to take up the proton. The mixture was refluxed for 10 min and the solvent was allowed to boil off slowly while methanol was added to replace dichloromethane. The crystalline metal diporphyrin that precipitated was collected by filtration, washed with methanol, and dried in vacuo.

Acknowledgment. This work was supported in part by NSF (C.K.C.) and NIH (GM21156 G.R.E. and S.S.E.). C.K.C. thanks Dr. C.-B. Wang and Ismail Abdalmuhdi for synthetic efforts. S.S.E. thanks NSF for a Visiting Professorship for Women, 1984.

Supplementary Material Available: Additional experimental section for **1**, **2**, **4**, **5**, **10**, **10a**, **13**, **13a**, **16–19**, **24–32**, and **34–37** (12 pages). Ordering information is given on any current masthead page.